Visualizing Generalized 3*x*+1 Function Dynamics

Jeffrey P. Dumont[a], Clifford A. Reiter[b,*]
(preprint)
[a] 5B Hedgerow Drive, Hudson, NH 03051, USA
[b] Department of Mathematics, Lafayette College, Easton, PA 18042, USA

Abstract
The function that results in 3*x*+1 for odd integers *x* and half of *x* for even *x* has led to intriguing questions. The 3*x*+1 conjecture states that iteration of that function on positive integers eventually results in the value 1. We investigate many generalizations of that function to the complex domain and visualize the resulting dynamics using escape time, stopping time, and basin of attraction images. We will see beautiful, rich dynamics consistent with the conjecture. We see that some generalizations have relatively simple real dynamics, which may make them useful for analysis and we see a complex generalization where sequences of stable egg shaped regions appear in coefficient stopping time images that suggests remarkable patterns for such stopping time.

Keywords: Hailstone Numbers, Collatz Problem, Syracuse Problem

1. Introduction

The 3*x*+1 problem concerns questions about the iteration of a deceptively simple function on the positive integers. The 3*x*+1 function is a delightful function to introduce in a recreational mathematics context since there are easy to state, but difficult, unsolved conjectures about the behavior of the function. The 3*x*+1 function has been known by many names: the Hailstone function, the Collatz function, the Syracuse function and others. While the main conjectures regarding the function are unsolved, many results are known. We refer readers interested in the history and theory of the function to the classic expository paper [1] and the book [2].

In this paper, our goal is create and visualize the dynamics of suitable generalizations of the 3*x*+1 function. We will see that there are multitudes of interesting ways to generalize the function to a complex domain where we will show the dynamics in a several ways. Escape time is the most commonly used technique for illustrating the behavior of complex valued maps such as those used to create the classic Mandelbrot and Julia sets. Basins of attraction are often used to observe the behavior of convergent iterative methods, such as Newton's method. Such images make apparent regions with similar long term behavior which gives insight into the dynamics of the function [3-7]. We will create images of both escape time and basins of attraction for generalizations of the 3*x*+1 function. However, we will also consider stopping time images since stopping time has been of great interest to people studying the 3*x*+1 function. There are three well-established senses of stopping time that we will consider, generalize, and visualize.

The 3*x*+1 function, which we will denote as T, is most elegantly defined on a positive integer *x* as follows.

---
[*] *E-mail addresses:* dumontj@lafayette.edu (J. P. Dumont), and reiterc@lafayette.edu (C. A. Reiter)

$$T(x) = \begin{cases} \dfrac{x}{2}, & \text{if } x \equiv 0 \bmod 2 \\ \dfrac{3x+1}{2}, & \text{if } x \equiv 1 \bmod 2 \end{cases} \qquad (1)$$

We can use that definition of T to compute T(5)=8, T(8)=4, T(4)=2, T(2)=1, and T(1)=2. Thus, iteration of T on 5 leads to the repeating cycle (1,2).

We denote the kth iterate of T on x by $T^k(x)$. The 3x+1 conjecture is that all positive integers eventually reach the cycle (1,2) upon iteration. More formally, we have the following.

> ***The 3x+1 Conjecture.*** For all positive integers x there is a nonnegative integer k so that $T^k(x) = 1$.

As another example, consider iteration of T beginning on 27. In Table 1 we see that after 70 iterations, 1 is obtained, but along the way, $T^{45}(27) = 4616$, so we see large intermediate values may occur.

2. Two Fundamental Generalizations
We will generalize the 3x+1 function in a manner that is consistent with its behavior on the positive integers but so that the generalizations are well defined for complex arguments. In this section we introduce two fundamental generalizations. In later sections we will see that there are multitudes of other interesting generalizations beyond these two.

In the paper of Terras [8] it was noted that the 3x+1 function T(x) can be rewritten in the form

$$T(x) = \frac{3^{\mathrm{mod}_2(x)} x + \mathrm{mod}_2(x)}{2} \qquad (2)$$

where $\mathrm{mod}_2(x)$ denotes a function that is 0 on the even integers and 1 on the odd integers. This form for T gives rise to the remainder representation for T, which plays an important role in the theory of the 3x+1 function. We will discuss this representation in the next section.

If we have any complex valued function which is 0 on the even integers and 1 on the odd integers, then that will give a generalization of $\mathrm{mod}_2(x)$. Then, using Equation (2) we in turn get a generalization of T(x) to the complex plane. Our choice for the modulo 2 function for our fundamental generalizations is the following.

$$\mathrm{mod}_2(x) = \sin^2\left(\frac{\pi x}{2}\right) \qquad (3)$$

This function has smooth oscillations between 0 and 1 on the real line, it is well defined for complex arguments, and it has complex derivatives of all orders.

k	$T^k(27)$	$\lambda_k(27)$
0	27	1
1	41	1.5
2	62	2.25
3	31	1.125
4	47	1.6875
⋮		
43	2051	70.2213
44	3077	105.332
45	4616	157.998
46	2308	78.999
47	1154	39.4995
⋮		
57	92	3.12447
58	46	1.56224
59	23	0.78111
60	35	1.17168
61	53	1.75752
⋮		
68	4	0.12357
69	2	0.06178
70	1	0.03089
71	2	0.04634
72	1	0.02317

Table 1. Some values of $T^k(27)$ **and** $\lambda_k(27)$**.**

Secondly, Chamberland [2,9] interpolates the two cases in the Equation (1) definition of T(x) using sine and cosine squared. Using our notation for $\mod_2(x)$, we can write the function he gives as follows.

$$C(x) = \frac{x}{2}\left(1 - \mod_2(x)\right) + \frac{3x+1}{2}\mod_2(x) \tag{4}$$

Notice it matches the definition in Equation (1) for even and odd integers and it is smooth in the complex plane. Also, using Equation (3), this simplifies to

$$C(x) = \frac{1}{4}\left(1 + 4x - (1+2x)\cos(\pi x)\right).$$

Thus T(x) and C(x), as defined in Equations (2)-(4) are two generalizations of the 3x+1 function to the complex plane. When viewing the 3x+1 function on integers, we can use either C(x) or T(x) since they are identical on the integers. In fact, their MacLaurin series agree to degree 3 and all even degree coefficients are the same. However, they are different functions and while there are similarities, we will see their dynamics are different.

While we concentrate on T(x) and C(x) when we introduce the visualization methods, we will consider other generalizations later. We will see that the dynamics of T(x) is somewhat simpler than those for C(x). In Section 7 we will consider several interesting alternative definitions for $\mod_2(x)$ and in Section 8 we consider another smooth generalization, the winding function W(x). Although it is complex along the real axis, images of its coefficient stopping time are especially intriguing. In Section 9 we will consider families of variants of T and C with the constants replaced by parameters.

3. Three Senses of Stopping Time

There are three types of "stopping time" that have been of interest to those studying the 3x+1 function [1,2,8]. Following the terminology in [1,8], these are called the total stopping time, the stopping time, and the coefficient stopping time. All three are interesting and important and we will visualize the behavior of each.

If the 3x+1 conjecture is true, then eventually each positive integer n reaches 1 upon iteration of T. It is natural to ask "how long does it take to reach 1?". The answer is called the "total stopping time". More formally, the *total stopping time* for a positive integer n is defined to be the smallest nonnegative integer k such that $T^k(n) = 1$ and it is defined to be infinity if there is no such k. Thus, the 3x+1 conjecture can be rephrased as the total stopping time conjecture: "for all positive integers, the total stopping time is finite".

We can generalize the total stopping time to complex x. However, we lose the connection with the 3x+1 conjecture and computational difficulties arise. We lose the connection with the 3x+1 conjecture because some non-positive integers are known never to reach 1. That can be seen since 0 is a fixed point. There are attractive negative cycles and we will see non-integer cycles too. We will consider such cycles in Section 6. If we "define" the total stopping time for T on complex x to be the smallest nonnegative integer k such that $T^k(x) = 1$ and infinity if there is no such k, we run into computational problems since when we do computations with finite precision complex numbers, exact tests of "equals 1" are not practical and are overly sensitive to roundoff. Therefore, we use "near 1", up to fuzz of about 10^{-14}, as our test. While the choice of fuzz is simply the

default used by our programming language, since 1 is part of an attractive cycle, we expect the qualitative behavior to be independent of the choice of fuzz. Likewise, we "define" the total stopping time for C on x to be the smallest nonnegative integer k such that $C^k(x)$ is near 1 and infinity if there is no such k.

Next we define plain stopping time (without an adjective like total). The *stopping time* for a positive integer n is defined to be the smallest nonnegative integer k such that $T^k(n) < n$ and *the stopping time* is defined to be infinity if there is no such k. Of course, if the stopping time is finite for the integers $n \geq 2$, then the 3x+1 conjecture would be true, since repeatedly reducing the size of the eventual iterates would lead to a decreasing subsequence and hence would eventually lead to 1. Conversely, if the 3x+1 conjecture is true, each integer $n \geq 2$ eventually reaches 1, which is smaller than n, and hence has finite stopping time. Therefore, the 3x+1 conjecture is equivalent to the finite stopping time conjecture: "all integers $n \geq 2$ have finite stopping time". Remarkably, while little is known about the total stopping time, quite a lot is known about the stopping time [1,2,8].

It is natural to define the *stopping time* for T on complex x to be the smallest nonnegative integer k such that $\left|T^k(x)\right| < |x|$ and define the *stopping time* to be infinity if there is no such k. A similar definition can be made for the stopping time for C on complex x. Testing the inequality for stopping time is not as computationally troublesome as testing "equals 1". Thus, stopping time has advantages over the total stopping time for computational, as well as theoretic reasons.

The third sense of stopping time is the coefficient stopping time. Before we define it, we state the remainder representation theorem. Let n be a positive integer and define the parity function, $z_k(n)$, the coefficient function $\lambda_k(n)$, and the remainder function $\rho_k(n)$ as follows.

$$z_k(n) = \mathrm{mod}_2(T^k(n)) , \tag{5}$$

$$\lambda_k(n) = \frac{3^{z_0(n)+z_1(n)+...+z_{k-1}(n)}}{2^k} , \text{ and} \tag{6}$$

$$\rho_k(n) = \frac{\lambda_k(n)}{2}\left(\frac{z_0(n)}{\lambda_1(n)} + \frac{z_1(n)}{\lambda_2(n)} + ... + \frac{z_{k-1}(n)}{\lambda_k(n)} \right). \tag{7}$$

Theorem (Terras). Let n be a positive integer and $z_k(n)$, $\lambda_k(n)$, and $\rho_k(n)$ be defined as above, then

$$T^k(n) = \lambda_k(n)n + \rho_k(n) . \tag{8}$$

The theorem can be shown by induction along with using the fundamental formula for T given in Equation (2). Since $\rho_k(n) > 0$, it is clear that if $T^k(n) < n$ then it must be true that $\lambda_k(n) < 1$ (but there is no obvious reason why the converse would hold).

The *coefficient stopping time* for n is defined to be the smallest nonnegative integer k such that $\lambda_k(n) < 1$ and the *coefficient stopping time* is infinity if there is no such k. The above remark implies that the coefficient stopping time is less than or equal to the stopping time. Remarkably, it is conjectured that they are equal. That is, the

coefficient stopping time conjecture states that "for all integers $n \geq 2$, the stopping time is the same as the coefficient stopping time". The coefficient stopping time can be extended to complex arguments; however, we defer that until Section 5.

Consider the three stopping times for $n = 27$. Referring to Table 1, we see that $T^{70}(27) = 1$ and since this is the first time 1 occurs, the total stopping time of 27 is 70. Also notice $T^{59}(27) = 23$ and this is the first time an iterate drops below 27, hence the stopping time of 27 is 59. Lastly, notice $\lambda_{59}(27) = 0.78111$ and this is the first time that $\lambda_k(27)$ is below 1, hence the coefficient stopping time of 27 is 59 which is the same as the stopping time.

4. Visualizing Escape and Stopping Time for $T(x)$ and $C(x)$

In Section 2 we saw that $T(x)$ and $C(x)$ were smooth generalizations of the $3x+1$ function to the complex plane. Since these functions involve $\text{mod}_2(x)$, which involves the sine, these functions grow exponentially in the imaginary direction. In fact, T is doubly exponential. Thus, we expect iteration of T and C to yield overflow away from the real axis. However, the $3x+1$ conjecture being true would imply that all positive integers are attracted to the cycle (1,2), and hence we expect iterates to remain finite near positive integers. Thus, in images of escape time and stopping time, we see how those conflicting properties resolve themselves. Escape time images use colors to show how quickly the computations get huge. In contrast, stopping time and total stopping time images show how long it takes for the behavior to be good (reduced in magnitude or near 1, respectively).

Figure 1 shows escape time, stopping time and total stopping time for $T(x)$. Each image in those figures corresponds to the portion of the complex plane with $-6 \leq \text{Re}(x) \leq 6$ and $-2 \leq \text{Im}(x) \leq 2$. The hue of each pixel corresponds to different escape or stopping times for the corresponding complex number. Time equaling 1 corresponds to red, 2 to orange, 3 to yellow, and so on until 11 is used for magenta. That color sequence is then recycled with slightly reduced intensities until time 254, which is the maximal time we computed. In the escape time images, black corresponds to points that do not escape where escape is defined by magnitude exceeding 10^{10}. In the stopping time images, white corresponds to points that exceeded machine precision while black corresponds to points that remained bounded, but which never satisfied the stopping condition.

Notice that the escape time image, shown at the top of Figure 1, shows black on the real axis where the integers appear. The red and orange away from the real axis correspond to rapidly growing computations. However, notice the rich fractal structure of the black regions.

On the other hand, the stopping time image for $T(x)$, shown in the center of Figure 1, is white away from the real axis, due to blow up. It is red near the even integers, since the stopping time is 1 there (except at an isolated pixel at 0). In between, we see white near the axis intertwined with bounded behavior (some other hue) with rich structure near the odd integers.

As expected, the total stopping time image, shown at the bottom of Figure 1, is white where the escape time was not black. The only large regions that are not black or white appear along the positive real axis. It is not surprising that along the negative real

axis there is black since there are attractive negative fixed points and cycles. Note that stopping time is far more "stable" than the total stopping time. Observe the red stopping time regions overlap considerable white and black in the total stopping time images. This corresponds to points that get smaller on a first iteration, but blow up or stay bounded (but do not get near 1) under function iteration.

Figure 2 shows escape time, stopping time and total stopping time for C(x). The comments are quite similar to those for Figure 1, but the shape of the fractal regions are different and the regions where the stopping time has a finite value seem to be rounder and smaller than similar regions for T(x).

Figure 3 shows zooms centered on 27 for the stopping time of T(x). The images in that figure have width 3×10^{-m}, with $m = 0, 1, 2$ for the images on the left side and with $m = 4, 5, 6$ for the images on the right side. Since the stopping time of 27 is 59, we expect that a zoom centered on 27 would eventually show nothing but the color associated with 59, a shade of magenta. The first image shows two huge red regions associated with 26 and 28. It is clear that there is a pattern with suggestions of symmetry, near the center. As we zoom in by a factor of 10, we get image 2 on the left, which suggests interesting symmetry around 27. A further zoom by a factor of 10, the bottom left image, shows symmetry doubling and the magenta region we expect around 27 prominently appears. However, it is clearly not centered around 27, which is at the middle of each image. The upper right image is a further zoom by a factor of 100 where we see that 27 is quite near the left edge of the magenta region. Two more zooms, shown on the right, show that eventually 27 does fall into the interior of the magenta region. An obvious question is where is the magenta region centered? Estimates from the images suggest that the center of the magenta region containing 27 is centered at approximately 27.003375 and the left edge of that region is on the real axis near 26.9999995. Thus, 27 is at the edge up to 4 orders of magnitude.

Images extended to $-30 \leq \text{Re}(x) \leq 30$, but at lower resolution, appear at [10] for a few of our figures, including those in Figure 1.

5. Coefficient Stopping Time

Recall that for a positive integer n, the coefficient stopping time was the smallest positive integer such that $\lambda_k(n) = \dfrac{3^{z_0(n)+z_1(n)+...+z_{k-1}(n)}}{2^k} < 1$. When generalized to complex arguments, we need to make the numbers real in order to do the comparison. Using the complex magnitude of $\lambda_k(n)$ seems to be a good choice. However, we could alternately take the magnitude of each $z_j(n)$ or we can even take the magnitude of n. However, the last two choices would seem to make better sense with corresponding variants of T(x) which we will describe below. Thus, we define the coefficient stopping times for T(x), T*(x) and T**(x) as follows. These stopping times are the smallest positive integer k such that the following hold, and are infinite if there is no such k.

(T) $\quad \left| \dfrac{3^{z_0(x)+z_1(x)+...+z_{k-1}(x)}}{2^k} \right| < 1$ upon iteration of $T(x) = \dfrac{3^{\text{mod}_2(x)} x + \text{mod}_2(x)}{2}$ upon x;

(T*) $\quad \dfrac{3^{z_0^*(x)+z_1^*(x)+...+z_{k-1}^*(x)}}{2^k} < 1$ upon iteration of $T^*(x) = \dfrac{3^{|\mathrm{mod}_2(x)|}\,x + \mathrm{mod}_2(x)}{2}$ upon x and

where $z_k^*(x) = \left|\mathrm{mod}_2(T^{*k}(x))\right|$;

(T**) $\quad \dfrac{3^{z_0^{**}(x)+z_1^{**}(x)+...+z_{k-1}^{**}(x)}}{2^k} < 1$ upon iteration of $T^{**}(x) = \dfrac{3^{\mathrm{mod}_2(|x|)}\,x + \mathrm{mod}_2(x)}{2}$ upon x

and where $z_k^{**}(x) = \mathrm{mod}_2\left(\left|T^{**k}(x)\right|\right)$;

Note that we might consider coefficient stopping time for other generalizations of the 3x+1 function such as C(x); however, that seems unnatural since there are no apparent analogues of the representation theorem for C(x). However, there are starred and double starred analogues of the remainder representation theorem corresponding to T* and T**. Of course, T* and T** are not differentiable.

Figure 4 shows the coefficient stopping time for T, T*, and T** where $-6 \le \mathrm{Re}(x) \le 6$ and $-2 \le \mathrm{Im}(x) \le 2$. The colors are as in the previous figures. Observe that around the even integers there are round red regions (where the coefficient stopping times are 1). In between, there are fractal behaviors that appear remarkably different in these three cases. The images for T* and T** have regions which appear chaotic.

6. Basins of Attraction

We will next visualize the basins of attraction for T(x) and C(x). That is, we want to color points that are attracted to the same cycles with the same color. This also raises computational issues. We do not want to assume we know the cycles that exist ahead of time, so carefully chosen representatives need to be gathered dynamically. However, cycles can, and do, shadow one another making it difficult to distinguish slow convergence to one cycle from convergence to a nearby cycle. Nonetheless, these experiments yield a wealth of information about the cycles that appear and what points go where. Thus, in spite of the computational difficulties, these are valuable experiments.

Figure 5 shows the basins of attraction for T(x) and C(x) along with a zoom near 1 for each. The top image shows the basins for T(x) for $-6 \le \mathrm{Re}(x) \le 6$, $-2 \le \mathrm{Im}(x) \le 2$ and the middle left image is a zoom centered on 1 with width 0.3. The bottom image shows the basins for C(x) for $-6 \le \mathrm{Re}(x) \le 6$, $-2 \le \mathrm{Im}(x) \le 2$ and the middle right image is a zoom centered on 1 with width 0.3. Each hue that appears corresponds to a basin and within each basin, the shade indicates the number of steps, modulo 3, required to obtain the cycle within tolerance 10^{-12}. Increasing iteration count corresponds to moving from light to medium to darkest bands within that shade.

In Table 2 we see the basins and the colors used for each basin for T(x) found by our computations. In each case we determined an expansion factor by taking the derivative of $T^p(x)$ at x where p denotes the period of the cycle and x is any element of the cycle. Thus, four of the basins are attracting while two are repelling. The basins for the fixed point near -1.15387, 0, and the 2-cycle (1,2) dominate. These correspond to blue, red and green, respectively. A small brown basin appears near -5.0109 and a single magenta pixel which appears at -5 is on the right edge of that brown basin. Of course, the green basins dominate around the positive integers, given the 3x+1 conjecture. The zoom

color	expansion factor	cycle
red	0.5	(0)
blue	0.469947	(-1.15387)
cyan	1.5	(-1)
green	0.75	(1, 2)
brown	0.703092	(-10.0157, -5.01091, -7.01408)
magenta	1.12501	(-10, -5, -7)

Table 2. Some Cycles for T(x).

color	expansion factor	cycle
red	0.5	(0)
blue	0.385708	(-1.27773)
cyan	1.5	(-1)
green	0.75	(1, 2)
yellow	-0.230754	(1.19253, 2.13866)
brown	0.0363716	(-10.0349, -5.046, -7.04531)
magenta	1.12504	(-10, -5, -7)
light green	0.0035933	(-136.002, -68.0033, -34.0035, -17.0027, -25.0038, -37.0048, -55.0051, -82.0042, -41.0056, -61.0052, -91.0038)
none	1.08086	(-136, -68, -34, -17, -25, -37, -55, -82, -41, -61, -91)

Table 3. Some Cycles for C(x).

near 1 shows the green basin dominates near 1 although red and blue features are scattered nearby.

In Table 3 we see the basins and the colors used for each basin for C(x) found by our computations. We see that there are five attractive cycles. In particular, there are attractive fixed points near -1.27773, 0 and 1 with basins having color blue, red and green. Again the 2-cycle (1,2) is attractive and shown in green. However, now there is a second attractive 2-cycle with approximate values (1.19253, 2.13866) shown in yellow. Notice that the dynamics along the positive real line intertwine these basins, but we only see green basins near the positive integers.

Note the dynamics of T(x) appear simpler along the positive real axis than those for C(x) since there is only one attractive postive cycle; namely, (1,2). Moreover, we saw in comparing Figure 1 and 2 that T(x) has larger regions that remain bounded and larger regions with small stopping time. Thus, it would seem that it would be worthwhile to investigate the real dynamics of T(x).

7. Alternate Generalizations of the Modulo 2 Function
We next consider other choices for the function $\mathrm{mod}_2(x)$ that was essential to creating the fundamental generalizations C(x) and T(x) of the $3x+1$ function given in Equations (2) and (4). Recall that the generalization of $\mathrm{mod}_2(x)$ was required to be defined for all complex numbers and have value 0 on the even integers and value 1 on the odd integers.

We have seen that $\mathrm{mod}_2(x) = \sin^2\left(\dfrac{\pi x}{2}\right)$ was a fine choice but we will consider
alternatives. In particular, Figure 6 will show images of the coefficient stopping time
when $\mathrm{mod}_2(x)$ in Equation (2), which defined T(x), is replaced by the following three
functions respectively. In each case, we define a function with the desired values on the
real line and then apply that function independently to the real and imaginary parts of x to
obtain our complex version of $\mathrm{mod}_2(x)$. The three functions are:

- the decimal remainder after division by 2
- a piecewise linear function, oscillating between 0 and 1 on the even and odd integers,
- the function $\sin^2\left(\dfrac{\pi x}{2}\right)$.

Notice that the first function is discontinuous. The corresponding image is shown
at the top of Figure 6 and straight boundaries appear. Indeed, the image appears to be
chopped into blocks. The second function is continuous, but has corners. It is a sawtooth
function that is not differentiable at the integer lattice points. The coefficient stopping
time is well behaved on disks around the even integer lattice points, but the behavior is
complicated in between. While there are still some straight edges along boundaries, the
image seems more coherent than the first. The third function is not the same as T(x) since
it is applied on the real and imaginary parts independently, not using the complex
argument to sine.

Notice we could equally well generalize C(x) since it is also dependent upon the
sense of $\mathrm{mod}_2(x)$, although we would not use coefficient stopping time in that case.
Consider further some of the myriad of generalizations of the 3x+1 function we could
define. We could use weighted averages of the different $\mathrm{mod}_2(x)$ functions, we could
use different versions in each of the two places where $\mathrm{mod}_2(x)$ is used in Equations (2)
and (4). We could take averages of the resulting C(x) and T(x) generalizations. Moreover,
adjustments by any function that is zero at the integers could be used. Thus, we could add
any finite sine series to another choice for $\mathrm{mod}_2(x)$. In particular, we could use

$\mathrm{mod}_2(x) = \sin^2\left(\dfrac{\pi x}{2}\right) + \sum_{k=1}^{K} c_k \sin(k\pi x)$. Indeed, in the next section we consider a natural,

smooth generalization of that form.

8. The Winding Function: A Smooth but Complex Generalization

The function $\mathrm{mod}_2(x) = \dfrac{1}{2}\left(1 - e^{i\pi x}\right) = \sin^2\left(\dfrac{\pi x}{2}\right) - \dfrac{i}{2}\sin(\pi x)$ is another smooth complex

$\mathrm{mod}_2(x)$ function. It is different from our fundamental choice by a complex sine term.
With that choice of $\mathrm{mod}_2(x)$, we define the *winding* 3x+1 *function* to be

$\mathrm{W}(x) = \dfrac{3^{\mathrm{mod}_2(x)} x + \mathrm{mod}_2(x)}{2}$. Since it gives complex values along the real axis, its

behavior is quite different from our other examples.

Figure 7 shows the escape time, stopping time, and basins of attraction for W(x).
The images are asymmetric because of the complex values. The integers appear in black

color	expansion factor	cycle
red	0.931048	(0)
magenta	2.34549	(-1)
green	0.570395	(1.52577j0.721276)
blue	0.813955	(3.10207j0.713843)
yellow	9.45387	(1,2)
cyan	1675.05	(-10, -5, -7)

Table 4. Some Cycles for T(x) with a Smooth Complex Modulo 2 Function.

regions of the escape time pictures. Some of them appear in quite small regions; for example, consider the center of the left edge where -6 appears.

The center image in Figure 7 shows the stopping time. The even integers appear inside the red dips, but the odd integers seem quite intertwined. A similar statement is true for the coefficient stopping time as we will see in the next image.

The bottom image in Figure 7 shows the basins of attraction. Only two basins of attraction are apparent. These are a green basin, corresponding to the complex fixed point 1.52577j0.721276, and the blue basin, corresponding to a complex fixed point 3.10207j0.713843. Table 4 summarizes some facts about the cycle structure. None of the other cycles capture more than a handful of pixels. The fixed point at 0 has an expansion factor near 0.931048. This is large enough that points converging to the origin have not done so within the required 254 iterations. Thus, some, if not all, of the black pixels correspond to points converging slowly to 0.

Figure 8 shows the coefficient stopping time for W(x) zooming in near 7. The coefficient stopping time for 7 is 7 and that coefficient stopping time is shown in cyan. The width of the images are 3×10^{-k} for k=0,1,2...,8. The images are arranged in reading order. Thus, in the upper left image, we see the red bulges that include 6 and 8. A zoom in toward 7 shows an edge near orange egg shaped regions, a further zoom shows an edge at a new angle near yellow egg shaped regions, then, in further zooms, we see light green, light green, green, green-cyan, green-cyan and finally cyan egg shaped regions. One can follow the coefficient stopping times from 1 (red) along a path through the zooms seeing it rise 12 and go back down to 7 in the final cyan egg. Since it takes eight orders of magnitude to find the cyan region where the coefficient stopping time is constant, it is not surprising that these computations are delicate.

However, there seems to be a path to the coefficient stopping time around 7 that could be described by the following. Travel from the red region onto the rainbow near 7. Turn right between the 1st and 2nd orange eggs. Then take a right between the 4th and 5th yellow egg, then another right between the 5th and 6th light green eggs, but aimed toward the 6th egg. Turn left after the 5th green egg and then right after the 4th green-cyan egg, aiming toward the 5th green-cyan egg. Then turn left onto the 4th cyan egg. This is the region surrounding 7. While that description is somewhat fanciful, it conveys the rich structure. Zooms near other points often have very similar behavior. However, we have observed that sometimes the final region is a band rather than an egg.

9. Nearby Families of Functions

We next briefly investigate the behavior of the $ax+1$ function. That is, we consider the behavior of the family of functions $T_a(x) = \dfrac{a^{\mathrm{mod}_2(x)}x + \mathrm{mod}_2(x)}{2}$ for

$\mathrm{mod}_2(x) = \sin^2\left(\dfrac{\pi x}{2}\right)$. Figure 9 shows the escape time for $-6 \leq \mathrm{Re}(x) \leq 6$ and

$-2 \leq \mathrm{Im}(x) \leq 2$ when a=1, 2, 2.5, 3, 4. As we should expect, the real axis is in a wide black region, corresponding to bounded behavior, for small values of a. the fractal structure becomes pronounced more quickly on the positive side of each image. By the time a=5, the orange region has gotten quite close to the axis. The basin of attraction near 0 seems to be quite persistent. Notice the striking amount of high iteration count colors near the positive real axis for a=3.5.

Animations showing the evolution of images of $T_a(x)$, and similar changes to C(x), are available at [10]. While the behavior of $T_a(x)$ may be somewhat simpler for $a \neq 3$, all of the images seem to illustrate nontrivial complex dynamics.

As our second family, we consider the functions $W_b(x) = \dfrac{3^{\mathrm{mod}_2(x)}x + \mathrm{mod}_2(x)}{2}$

where $\mathrm{mod}_2(x) = \sin^2\left(\dfrac{\pi x}{2}\right) + bi\sin(\pi x)$. Notice that $W_0(x) = T(x)$ while

$W_{-0.5}(x) = W(x)$. Figure 10 shows the escape time for $W_b(x)$ when b=0, -0.2, -0.48, -0.5, -0.51, -0.9. Notice that the first image is the same as the one for T(x), the second is similar, but distortion is clear, the next three are all quite close to W(x), and the last shows finite escape times dominating. This sequence shows there is a dramatic change in behavior for $W_b(x)$ when $W_{-0.5}(x) = W(x)$. This offers further evidence that the winding $3x+1$ function is worth further investigation.

10. On Implementation

The experiments described in this paper were done using programs written in J by the authors. We used Jsoftware 4.05d which is free. The web site for Jsoftware is [11]. Readers interested in duplicating some of these images can obtain J scripts from [10]. We offer below a few brief illustrations of our computations; we offer this so that we can briefly illustrate the experimental environment we used; also readers will have data allowing them to replicate and verify our computations; and we will point out a computational limitation of our experiments. We will not comment on the implementation details of the J expressions, but rather focus upon the results and usage.

First we implement our sense of modulo 2 from Equation (3). Applying it we see the correct results on 1, 2 and 3, a very tiny bit of round off error on 4, and the generalization to the noninteger 3.1.

```
   mod2a=: *:@(1&o.)@(1r2p1&*)

   mod2a 1 2 3 4 3.1
1 0 1 5.99864e_32 0.975528
```

Next, we implement the winding $3x+1$ function, $W(x)$, that we used in Section 8. Note it is complex valued at 3.1.

```
   mod2w=:  -:@(1:-_12&o.@o.)

   mod2w 1 2 3 4 3.1
1 0 1 0 0.975528j0.154508
```

We implement Equation (2) as an adverb that takes a sense of modulo 2 as a function argument and gives the resulting function $T(x)$. Here we see a few iterates of the $3x+1$ function on 7 and then on 7.02.

```
   T1=: 1 : '-:@((]+[* 3: ^ ]) u.) f.'

   mod2a T1^:(i.9) 7
7 11 17 26 13 20 10 5 8

   mod2a T1^:(i.7) 7.02
7.02 11.0181 17.0121 26.0078 13.0062 20.0072 10.0051
```

We denote our stopping time adverb by SIG. We see that the stopping time of 7, 7.1, and 27 are 7, 4, and 27 respectively. When we use the smooth complex version of modulo 2, we get a different stopping time for 7.1, which is typical for non-integral values. However, we also see that we were unable to correctly compute the stopping time at 27. This is not too surprising given the stopping time is 59 and 8 orders of magnitude were required, see Section 8, to focus around a stable coefficient stopping time region when it was 7. Nonetheless, this inability to compute the coefficient stopping time near 27 illustrates a computational limitation of using finite precision complex numbers.

```
   SIG=:1 : 0       NB. fct arg is "T"
sigs=.0 1&+@}: , u.@{:
sigl=.sigs^:((1&{ < 255"_)*. {. <:&| {:)^:_
(((~:>:)@{:*1&{)@sigl@(],0:,]) f. :: 0:)"0
)

   mod2a T1 SIG 7 7.1 27
7 4 59

   mod2w T1 SIG 7 7.1 27
7 5 0
```

Next we create a function that gives small arrays of inputs. Then we can apply our stopping time functions to that array. Notice results of 255 correspond to maximum iteration reached, results of 0 mean the computations became huge, and other results are the appropriate stopping times. Note the asymmetry of the stopping time for the mod2w

function. It is easy to take larger versions of the resulting arrays and turn them into images.

```
   zl_clur=: 4 : 0
w=.-~/9 o.y.
h=.-~/11 o.y.
(h*(i:%j.)<.0.5+x.*h%w) +/ ({.y.)+w*(i.%<:)1+x.
)

   ]z=: 4 zl_clur 0 2j1
   0j1     0.5j1     1j1     1.5j1     2j1
 0j0.5   0.5j0.5   1j0.5   1.5j0.5   2j0.5
     0       0.5       1       1.5       2
0j_0.5 0.5j_0.5 1j_0.5 1.5j_0.5 2j_0.5
   0j_1    0.5j_1    1j_1    1.5j_1    2j_1

   mod2a T1 SIG z
255   0   0 0 3
  1 255   0 0 1
255 255 255 2 1
  1 255   0 0 1
255   0   0 0 3

   mod2w T1 SIG z
  1   1 255   1 1
  1 255 255 255 1
255   0 255 255 1
255 255   0   4 1
  9   0   0  16 5
```

Lastly, we show how we created the $ax+1$ functions that we explored in Section 9. We show the values of the $3x+1$ function, the $5x+1$ function and the $2.1x+1$ function on 7 and 8.

```
   TX=: 1 : '-:@((]+[* (m."_) ^ ]) mod2a) f.'

   3 TX 7 8
11 4

   5 TX 7 8
18 4

   2.1 TX 7 8
7.85 4
```

Conclusion

We have seen that we can generalize the $3x+1$ function to the complex plane in a wide variety of ways. We can then visualize the dynamics of those functions using escape time, basins of attraction, and stopping time images. We noticed that T(x) has simpler dynamics than C(x) along the real axis. We saw the winding $3x+1$ function displayed remarkable sequences of stable egg shaped regions in zooms toward integers in the corresponding stopping time images. The intrigue of the $3x+1$ problem can be seen in these wonderful images, and they suggest T(x) and W(x) are worth further study.

References

[1]   J. C. Lagarias, The $3x+1$ problem and its generalizations, *The American Mathematical Monthly*, **92** (1985) 1-23.

[2]   G. J. Wirsching, *The Dynamical Systems Generated by the 3n+1 Function*, Lecture Notes in Mathematics 1681, Springer, Berlin, 1998.

[3]   R. L. Devaney, *Chaos, Fractals and Dynamics*, Addison-Wesley Publishing Co., New York, 1990.

[4]   B. B. Mandelbrot, *The Fractal Geometry of Nature*, W. H. Freeman and Co., New York, 1982.

[5]   H-O Peitgen, H. Jürgens, D. Saupe, *Chaos and Fractals*, Springer-Verlag, New York, 1992.

[6]   C. A. Pickover, ed., *Chaos and Fractals, A Computer Graphical Journey*, Elsevier, Oxford, 1998.

[7]   C. A. Reiter, *Fractals, Visualization, and J*, Jsoftware Inc., Toronto, 2000.

[8]   R. Terras, A stopping time problem on the positive integers, *Acta Arithmetica*, **XXX** (1976) 241-252.

[9]   M. Chamberland, A continuous extension of the $3x+1$ problem to the real line, *Dynamics of Continuous, Discrete, and Impulsive Systems*, 2 (1996) 495-509.

[10]   J. P. Dumont, C. A. Reiter, Complex dynamics of the generalized $3x+1$ function, web page: *http://www.lafayette.edu/~reiterc/3x+1/index.html* .

[11]   Jsoftware web page, *http://www.jsoftware.com* .
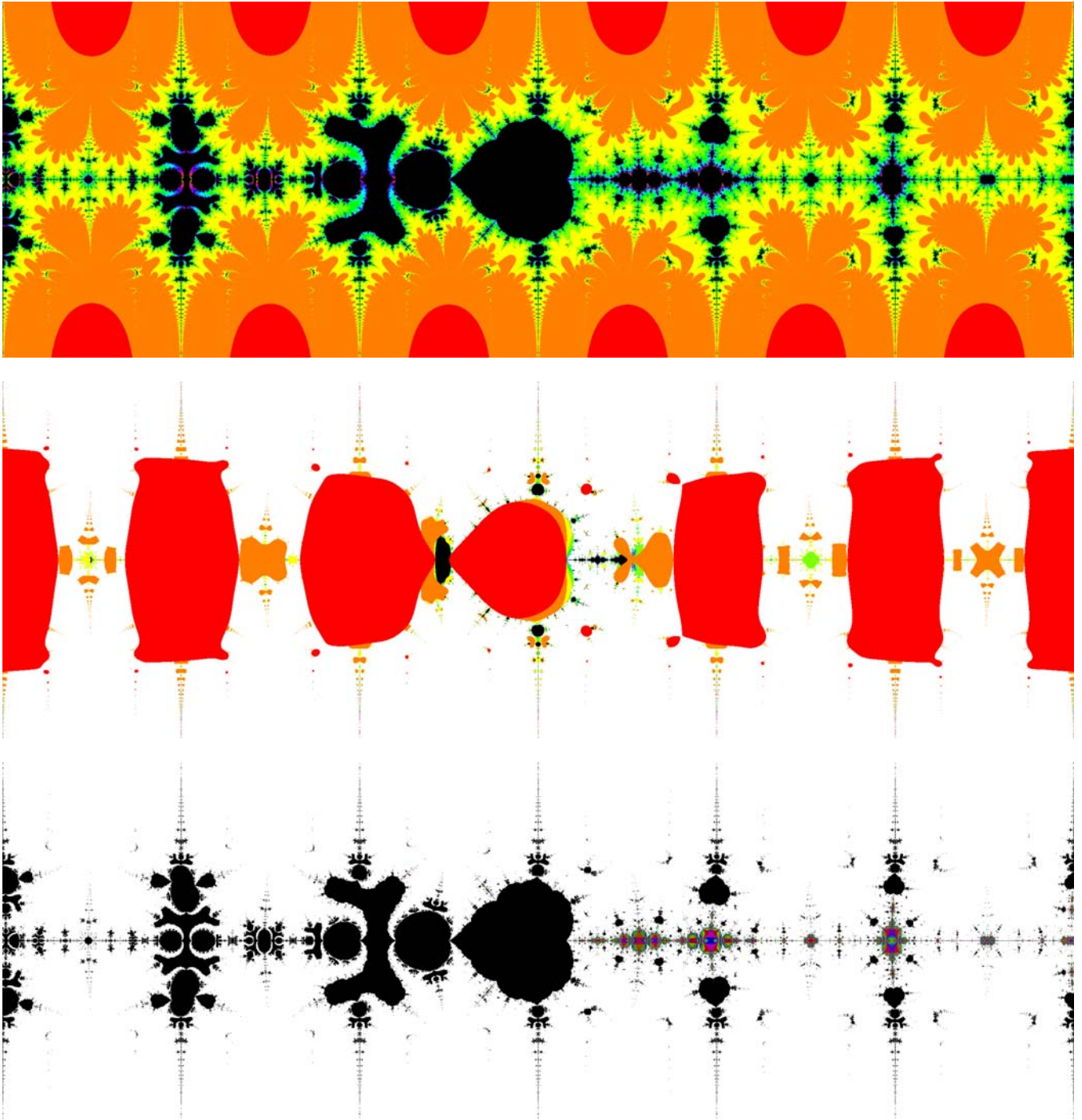
Figure 1. The escape, stopping time and total stopping time for T(x) where
$-6 \leq \mathrm{Re}(x) \leq 6$ and $-2 \leq \mathrm{Im}(x) \leq 2$.
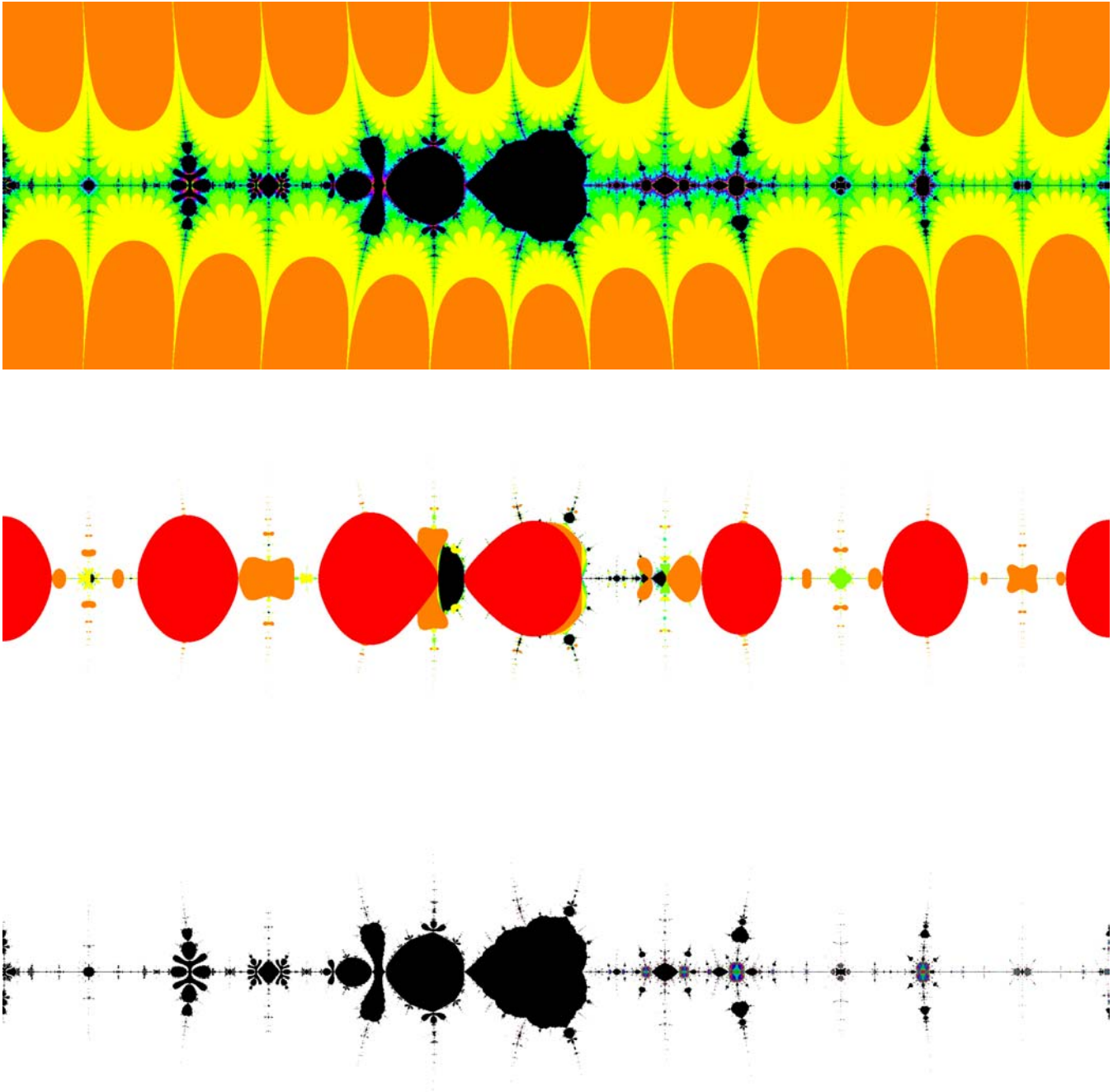
Figure 2. The escape, stopping time and total stopping time for C(x) where
$-6 \leq \mathrm{Re}(x) \leq 6$ and $-2 \leq \mathrm{Im}(x) \leq 2$.
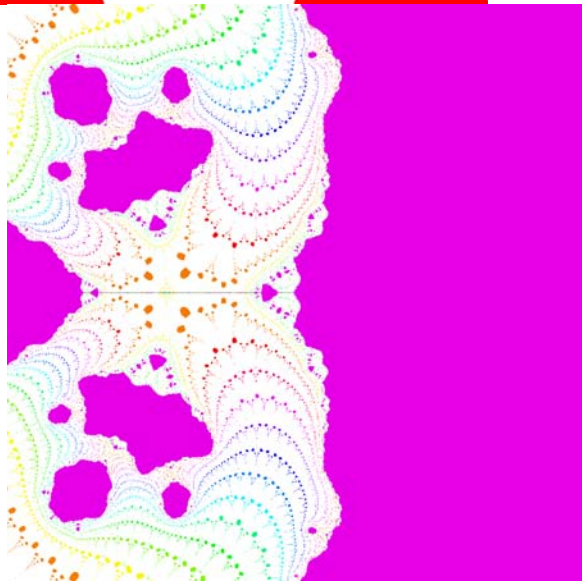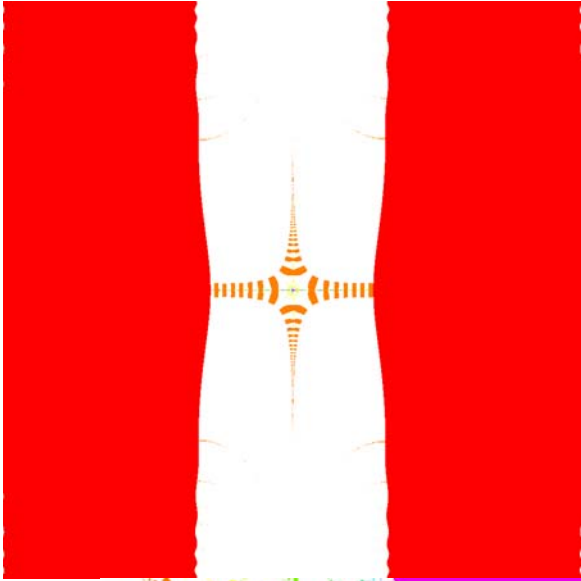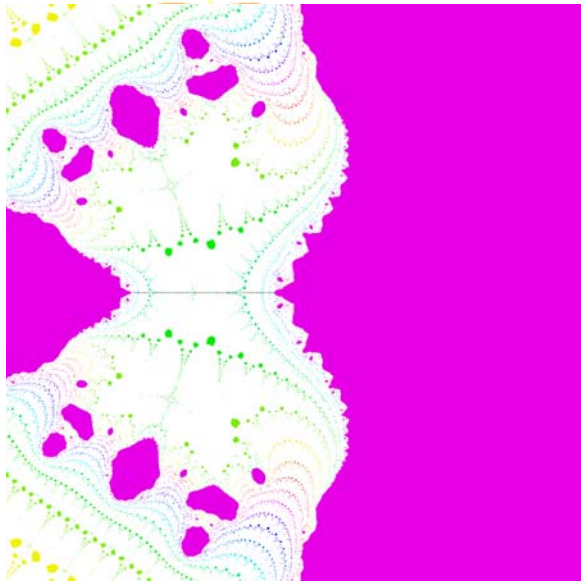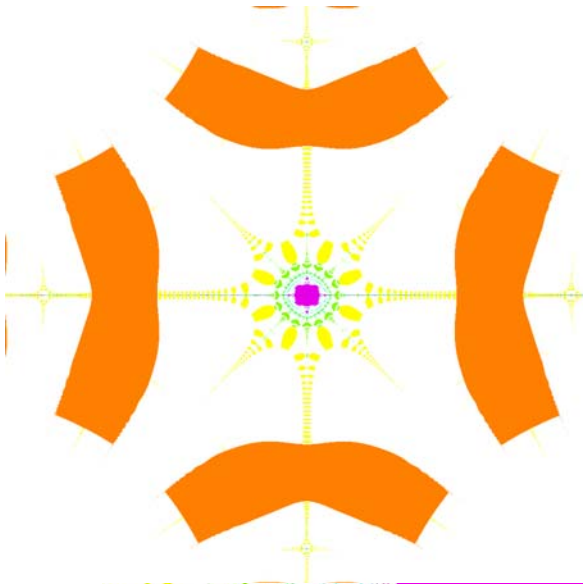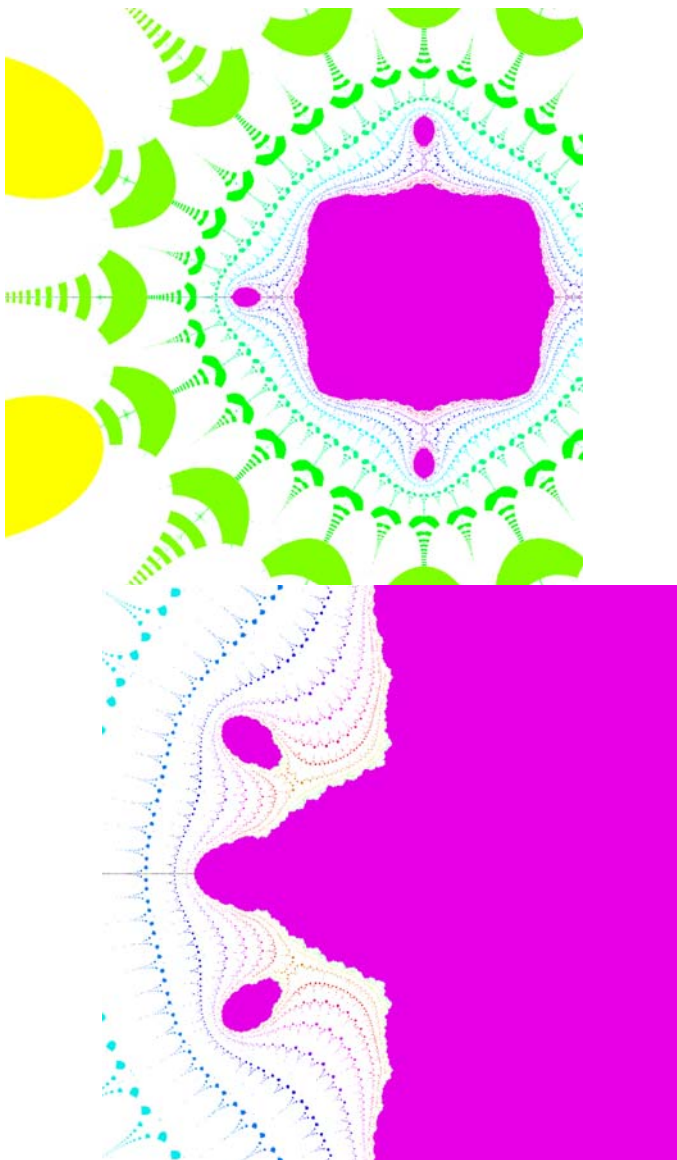
Figure 3. Zooms of the T(x) stopping time centered on 27 with width 3×10^{-m}, $m = 0,1,2,4,5,6$.
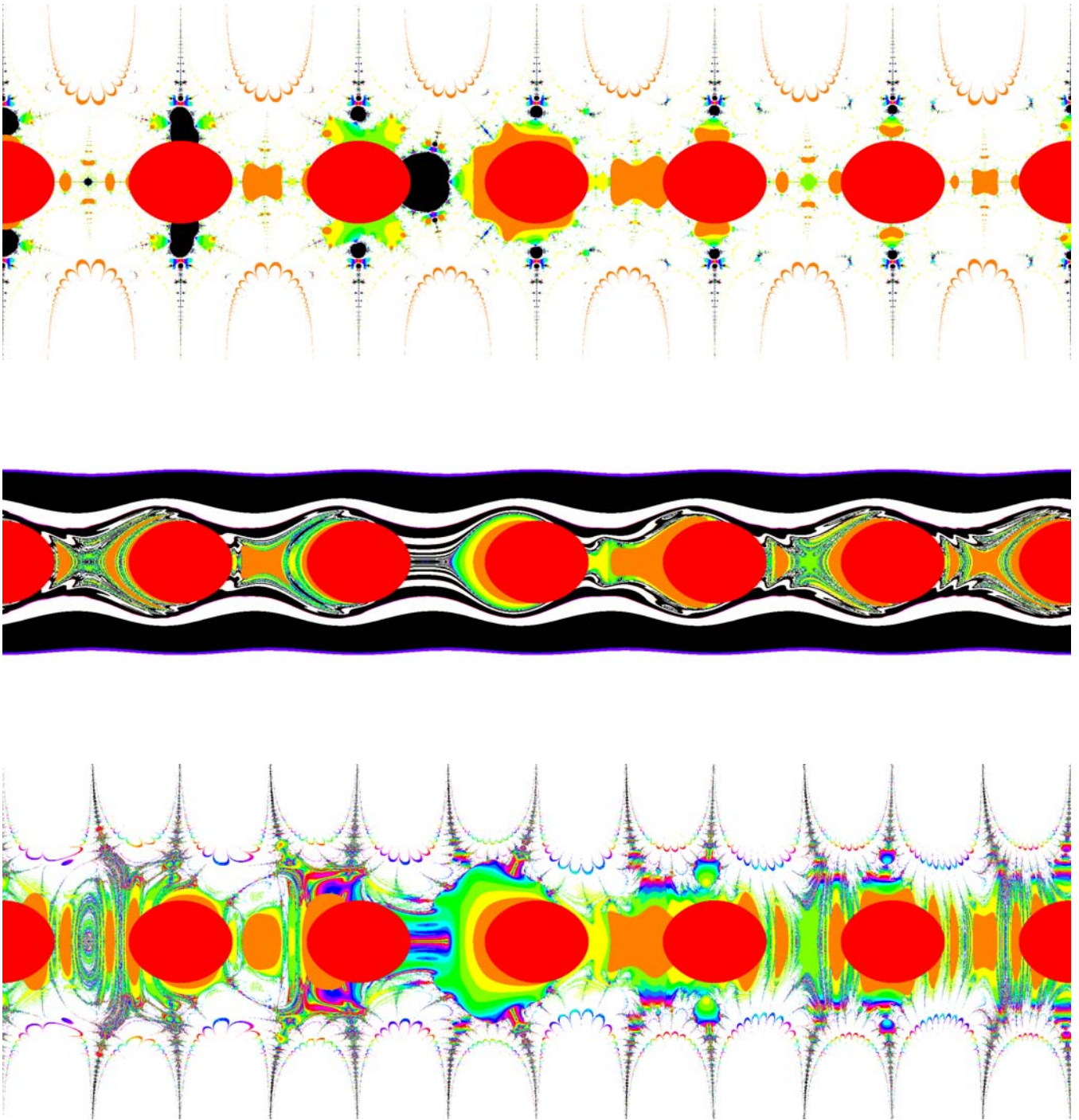
Figure 4. The coefficient stopping times for T(x), T*(x), and T**(x).
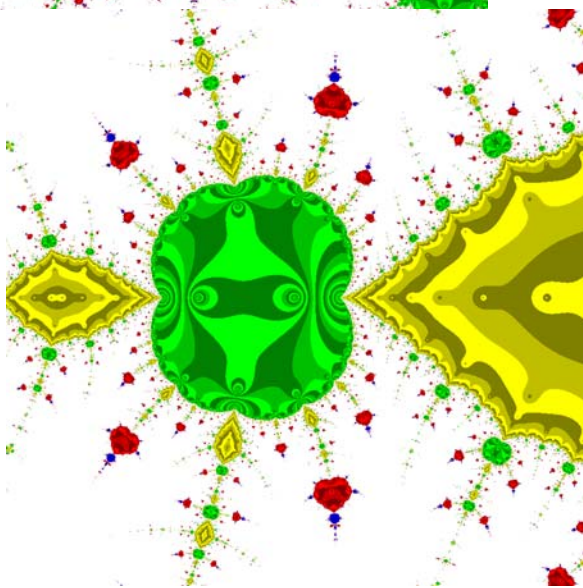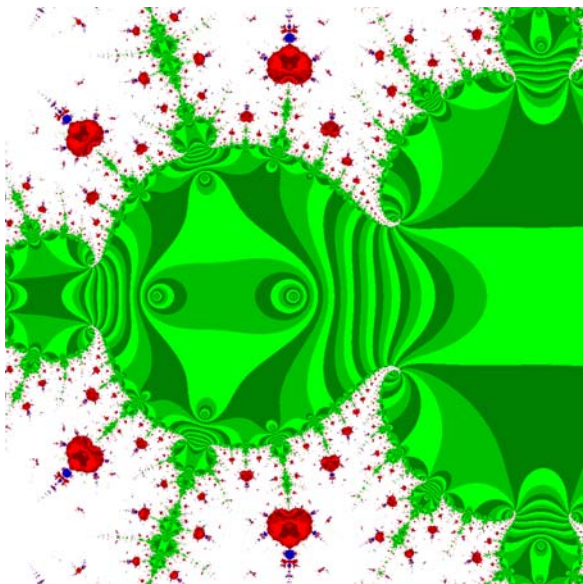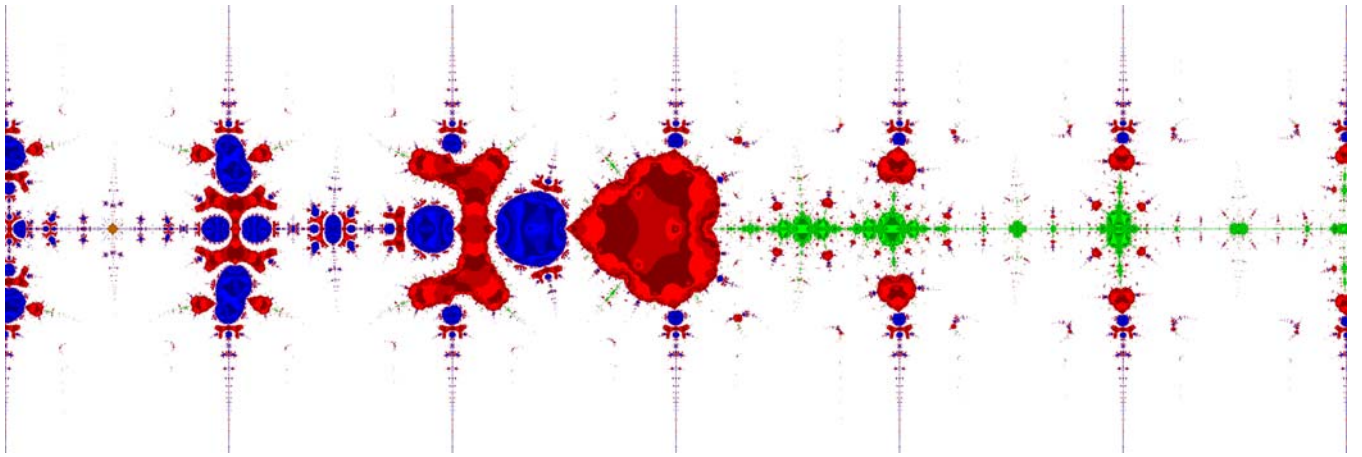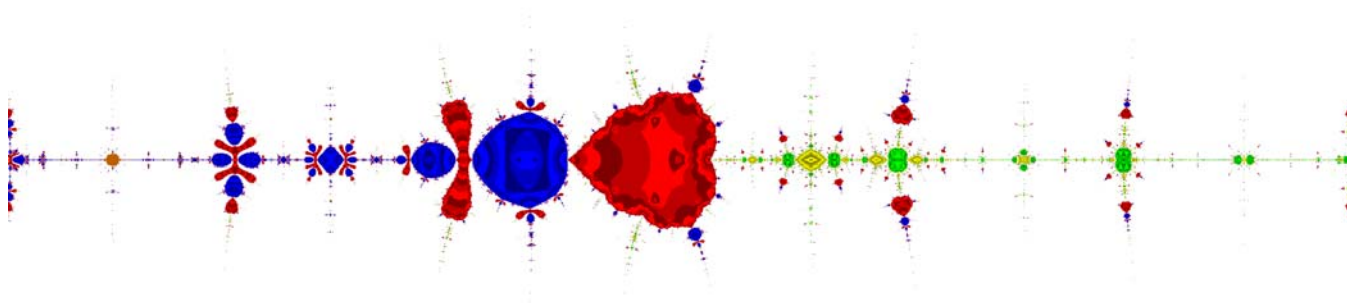
Figure 5. Basins of Attraction. Top: T(x) for $-6 \leq \mathrm{Re}(x) \leq 6$, middle-left: T($x$) zoom near 1, middle-right: C(x) zoom near 1, and bottom: C(x) for $-6 \leq \mathrm{Re}(x) \leq 6$.
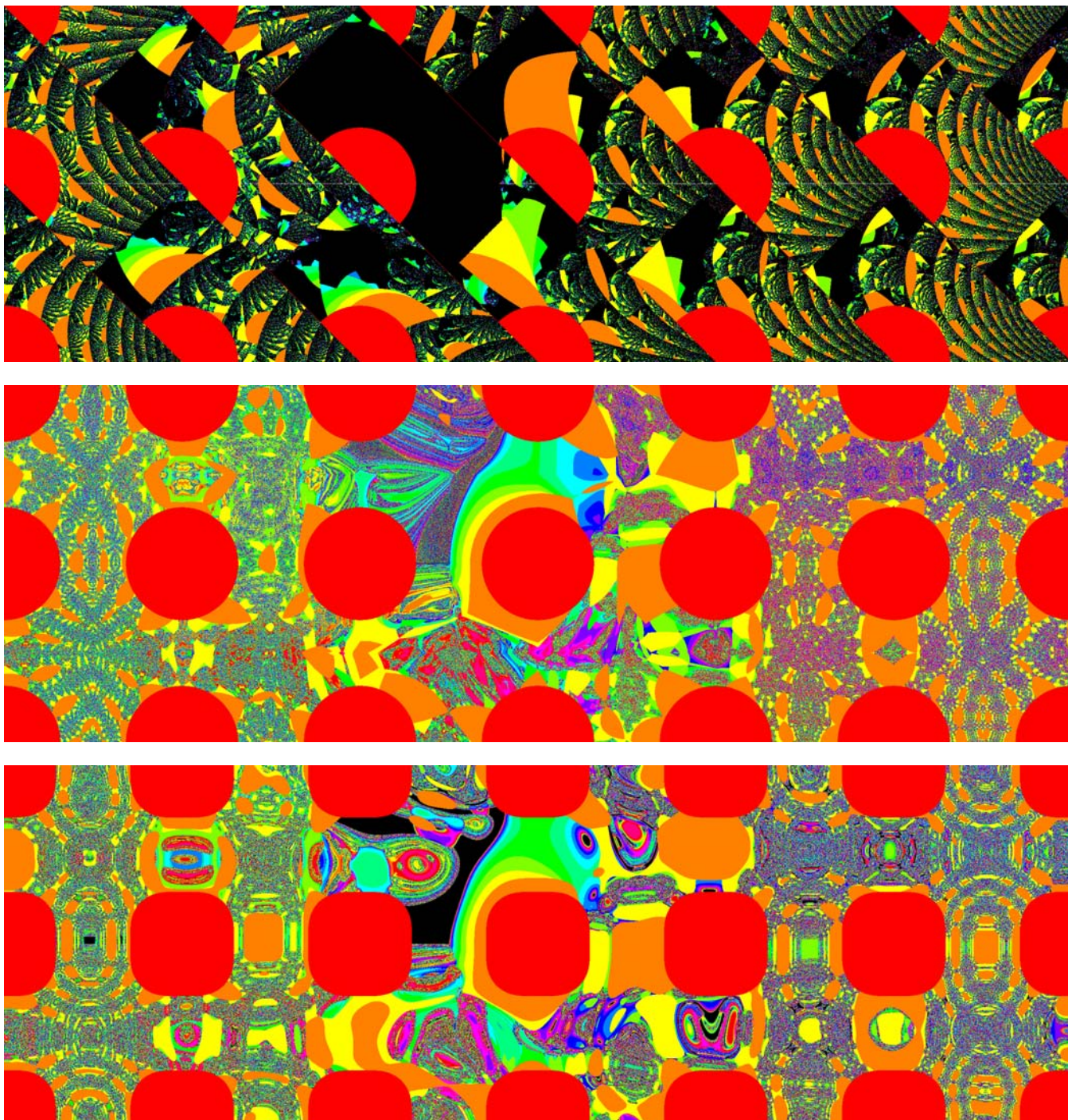
Figure 6. Coefficient stopping time for T(x) with mod$_2$(x) modified so real and imaginary parts are given by: remainder upon division by 2, a sawtooth function, and sine squared.
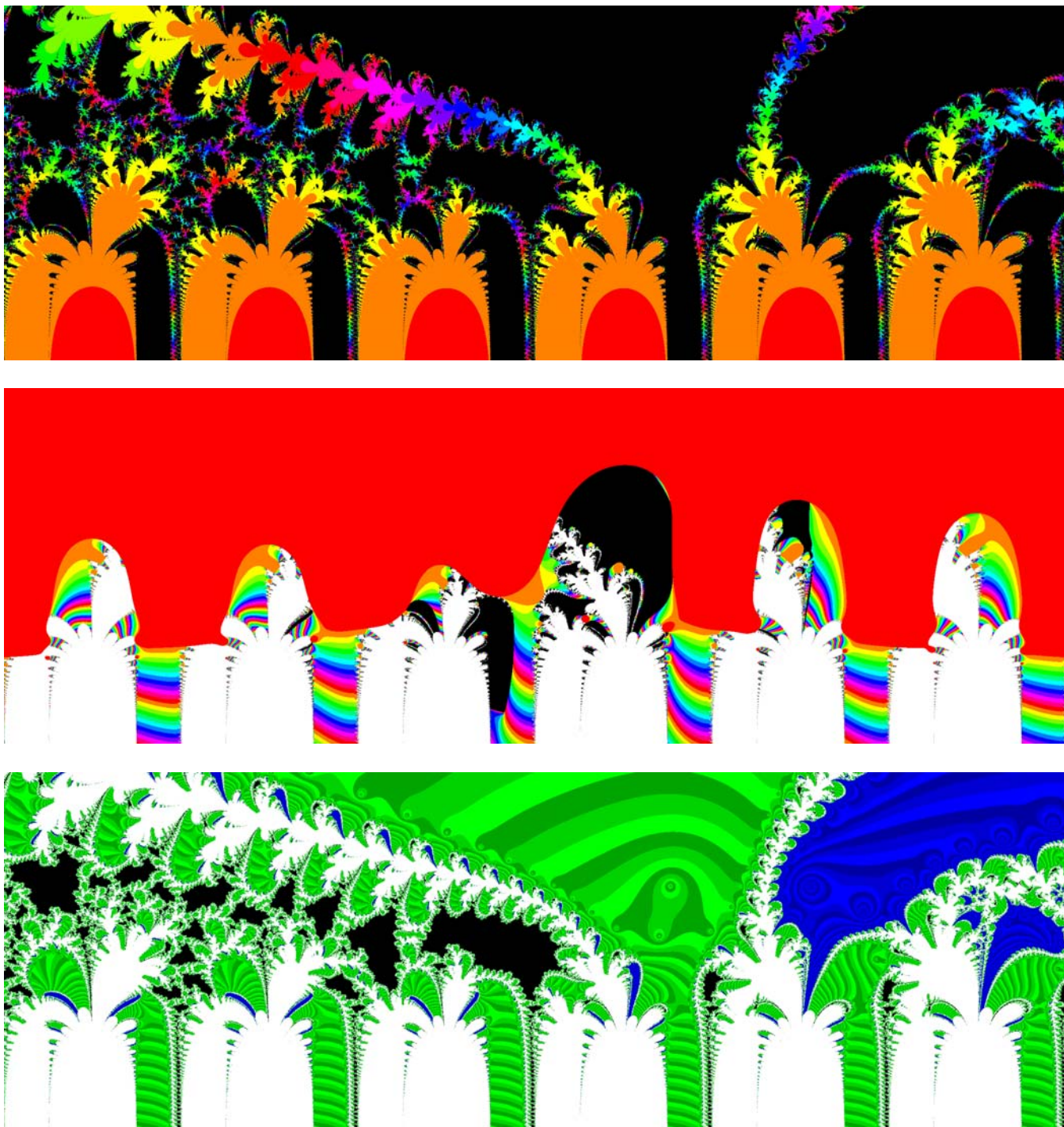
Figure 7. Escape time, stopping time, and basins of attraction for W(*x*), the winding 3*x*+1 function.
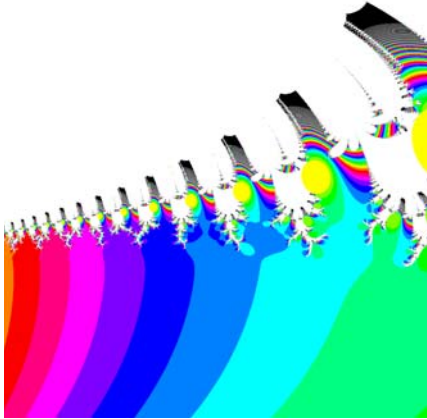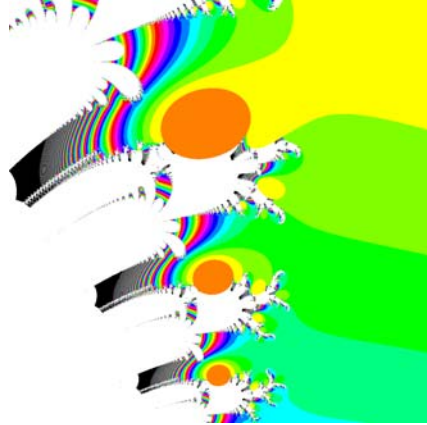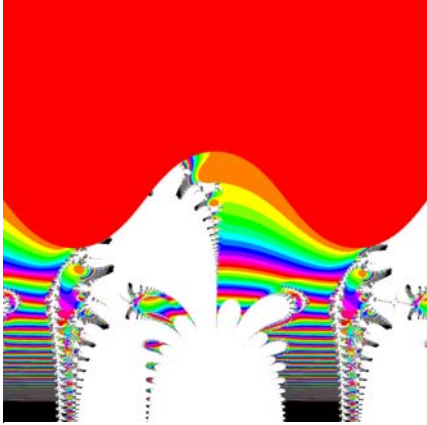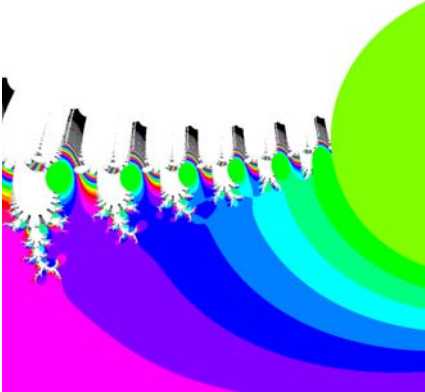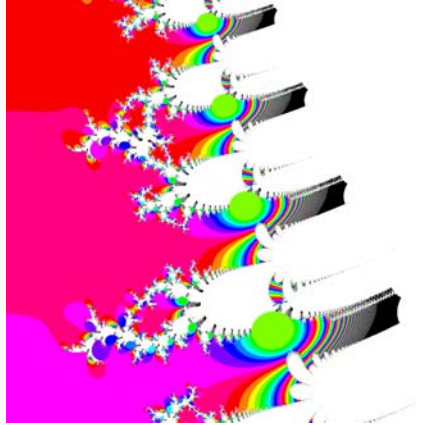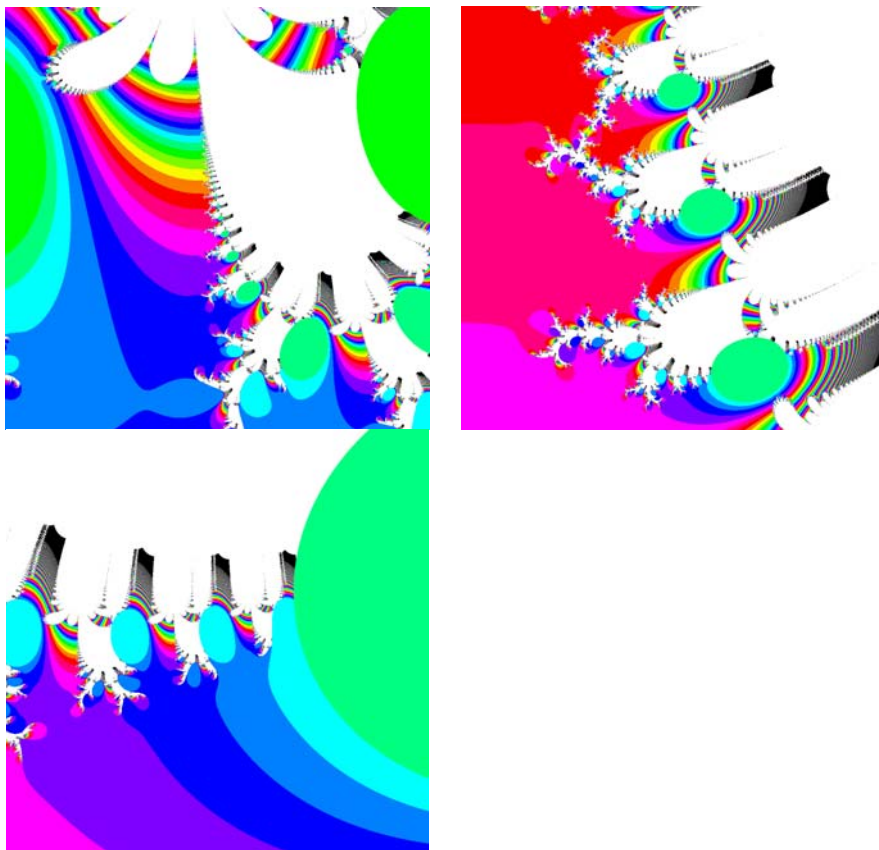
Figure 8. Coefficient stopping time for W(x) near 7.
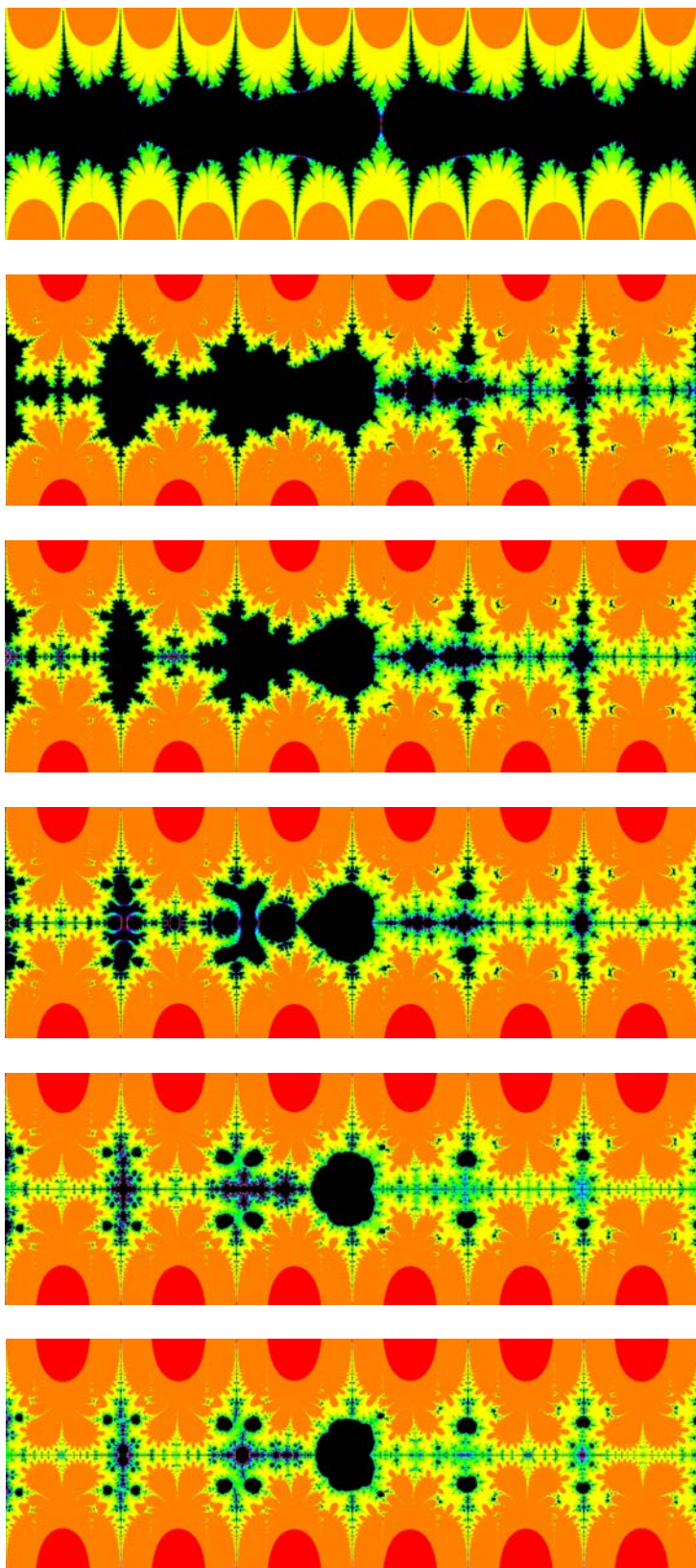
Figure 9. Escape time for the *ax*+1 function, *a*=1, 2, 2.5, 3, 4, 5.
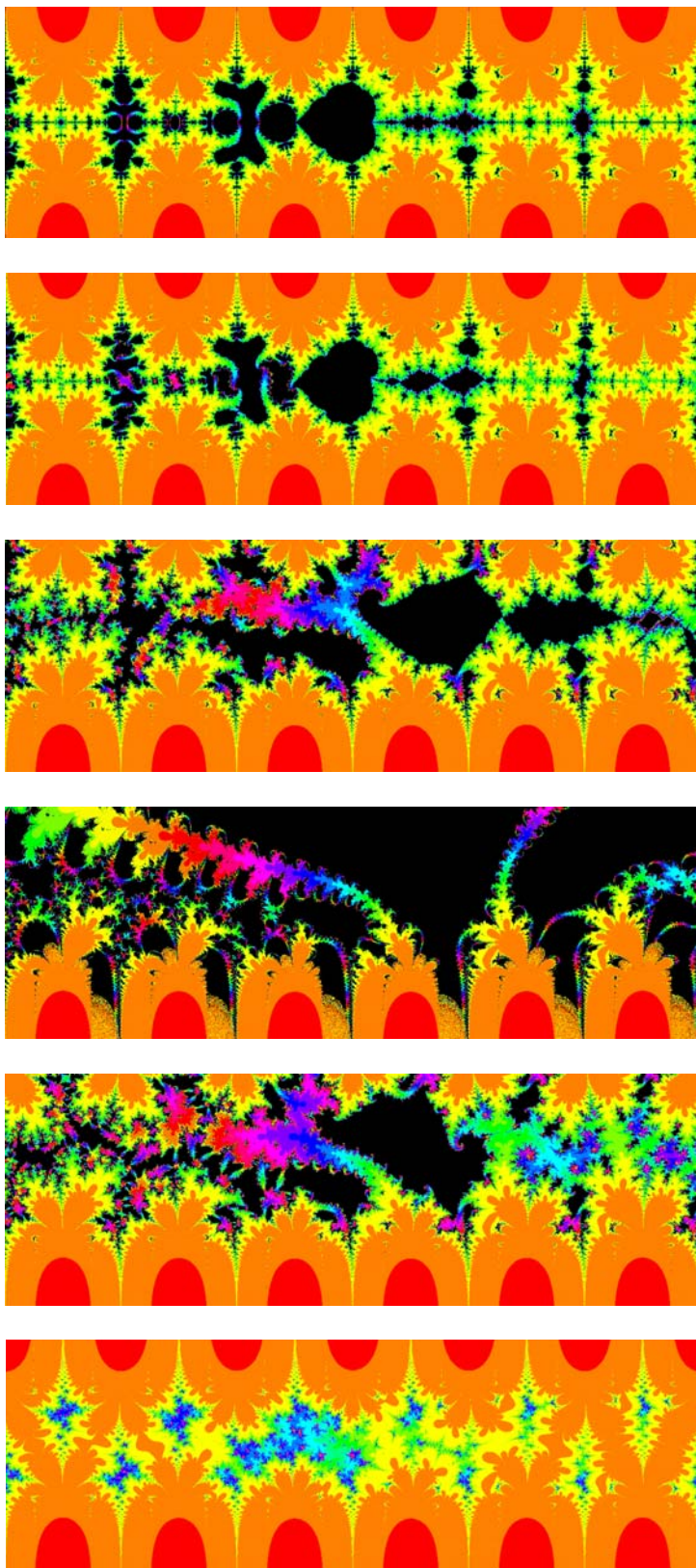
Figure 10. Escape time for $W_b(x)$ for b=0, -0.2, -0.48, -0.5, -0.51, -0.9.